PHYSICAL REVIEW C VOLUME 46, NUMBER 4 OCTOBER 1992

Multiple-scattering effects in quasielastic α-^{4}He scattering

Francis A. Cucinotta, Lawrence W. Townsend, and John W. Wilson
NASA Langley Research Center, Hampton, Virginia 23665
(Received 3 January 1992)

A multiple-scattering series for describing the quasielastic peak in nucleus-nucleus collisions is derived using the high-energy optical model. The effects of multiple knockout of target nucleons and internal excitation of the projectile are studied and found to be important for large energy loss and momentum transfers in inclusive α-^{4}He scattering at 7 GeV/c. An approximate evaluation of higher-order inelastic collision terms is considered for forward-peaked wave functions and is demonstrated to be accurate.

PACS number(s): 24.10.−i, 25.55.Ci

INTRODUCTION

Inclusive inelastic-scattering data for hadron-nucleus collisions are often described using the inelastic sum rule of Glauber and Matthiae [1]. In the original work [1], only the distribution in momentum transfer to the projectile in inelastic scattering is considered, using closure to sum over the target's final states. Additional considerations of energy conservation in multiple-scattering theory allow for a description of the projectile's energy loss [2–5] and the quasielastic peak in the cross section. In recent years inelastic-scattering data for light projectile nuclei have become available [6–8]. When compared with proton projectiles, we expect contributions from multiple scatterings to increase. Also, for energy transfers below pion production thresholds, the role that internal structure of the projectile plays is not clear when the quasifree picture of nearly free nucleon-nucleon collisions between projectile and target nucleons holds.

One approach to describing this data has been to consider the projectile as "elementary" and to modify the hadron-nucleus scattering expressions by using a rigid-projectile assumption, where the internal structure is neglected [4,9,10]. In this paper we follow a more fundamental approach by starting from the nucleus-nucleus scattering amplitude and formulating the inclusive cross section for the projectile when it receives both energy loss and momentum transfer without a change of state. Previously [11], we have shown that eikonal-approximate solutions to optical-model [12,13] coupled-channel equations, derived from Watson's form of the nucleus-nucleus scattering series, are equivalent to the Glauber-Matthiae model of the scattering amplitude [14]. The coupled-channel amplitudes appear as a matrix representation of the Glauber-Matthiae model. We begin with the eikonal coupled-channel amplitude in formulating the projectile energy-loss cross section. Assuming a mean field for coupling to diagonal states, we consider a multiple-scattering series for inclusive reactions. The leading-order correction for internal excitation of the projectile appears as an incoherent contribution to second-order terms.

We consider calculations for α-^{4}He reactions at 4 GeV. The importance of multiple scattering and internal projectile excitation are then analyzed by comparing to experiments. An approximate treatment of higher-order terms is considered for forward-peaked wave functions. Previously [15], the α-^{4}He inclusive reaction was analyzed using the Monte Carlo method, with the normalization of calculations fitted to experiments. An important conclusion was that the data could be explained by considering the incident α to elastically scatter on substructures of the target. For simplicity, we use uncorrelated single-particle wave functions in our calculations. Clustering effects could be considered in our analytic approach at a later data by introducing overlap functions in evaluating the target response function.

MULTIPLE INELASTIC COLLISION SERIES

In the Eikonal coupled-channel (ECC) model [11,12] the matrix of scattering amplitudes for all possible projectile-target transitions is given by

$$\bar{f}(\mathbf{q})=\frac{ik}{2\pi}\hat{Z}\int d^2b\, e^{i\mathbf{q}\cdot\mathbf{b}}\{e^{i\bar{\chi}(\mathbf{b})}-\bar{1}\}\ , \qquad (1)$$

where barred quantities represent matrices, $\mathbf{b}$ is the impact-parameter vector, $\mathbf{q}$ the momentum-transfer vector, and k the projectile-target relative wave number. In (1), $\hat{Z}$ is an ordering operator for the z coordinate, which is necessary only when noncommuting, two-body interactions are considered. The phase elements of $\bar{\chi}$ are defined by matrix elements of arbitrary projectile-target states of the operator

$$\hat{\chi}(\mathbf{b})=\frac{1}{2\pi k_{NN}}\sum_{\alpha,j}\int d^2q\, e^{i\mathbf{q}\cdot\mathbf{b}}e^{-i\mathbf{q}\cdot\mathbf{s}_\alpha}e^{i\mathbf{q}\cdot\mathbf{s}_j}f_{NN}(\mathbf{q})\ , \qquad (2)$$

where a spin-independent two-body amplitude is assumed and where α and j label the projectile and target constituents, respectively: $\mathbf{s}$ is the projection of the internal nuclear coordinate onto the impact-parameter plane, f_{NN} is the nucleon-nucleon (NN) amplitude, and k_{NN} is the NN relative wave number.

In treating inelastic scattering, we assume that the off-diagonal terms in $\bar{\chi}$, denoted by $\bar{\chi}_o$, are small compared with the diagonal one $\bar{\chi}_D$, and then expand $\bar{f}$ in powers of $\bar{\chi}_0$,

$$\bar{f}(\mathbf{q})=\frac{ik}{2\pi}\int d^2b\, e^{i\mathbf{q}\cdot\mathbf{b}}e^{i\bar{\chi}_D(\mathbf{b})}\sum_{m=1}\left[\frac{[i\bar{\chi}_o(\mathbf{b})]^m}{m!}\right] . \tag{3}$$

We also will make the assumption that the diagonal terms are all represented by the ground-state elastic phase χ. Using (3), we sum over target final states X (continuum) to find the inclusive angular distribution for the projectile when its mass remains unchanged as

$$\left.\frac{d\sigma}{d\Omega}\right|_{\text{in}}=\frac{k^2}{(2\pi)^2}\int d^2b\, d^2b'\, e^{i\mathbf{q}\cdot(\mathbf{b}-\mathbf{b}')}e^{i[\chi(\mathbf{b})-\chi^\dagger(\mathbf{b}')]}\sum_{X\neq 0}\sum_{m=1}\frac{1}{(m!)^2}\langle 0_P0_T|[i\hat{\chi}(\mathbf{b})]^m|0_PX\rangle\langle X0_P|[-i\hat{\chi}^\dagger(\mathbf{b}')]^m|0_P0_T\rangle . \tag{4}$$

Equation (4) allows only for a study of the momentum-transfer spectra of the projectile. In considering the projectile energy loss, energy conservation must be treated. Using continuum states for the target final state, energy conservation leads to

$$\left.\frac{d^2\sigma}{d\Omega\, dE_P'}\right|_{\text{in}}=\frac{k^2}{(2\pi)^2}\int d^2b\, d^2b'\, e^{i\mathbf{q}\cdot(\mathbf{b}-\mathbf{b}')}e^{i[\chi(\mathbf{b})-\chi^\dagger(\mathbf{b}')]}\sum_{m=1}^{A_T}W_m(\mathbf{b},\mathbf{b}',w) , \tag{5}$$

where E_P' is the energy of the projectile in the final state and w is the projectile energy loss. We define

$$W_m(\mathbf{b},\mathbf{b}',w)=\frac{1}{(m!)^2}\int\prod_{j=1}^{m}\left[\frac{d\mathbf{k}_j}{(2\pi)^2}\right]\delta(E_f-E_i)\langle 0_P0_T|[\hat{\chi}(\mathbf{b})]^m|0_p\mathbf{k}_j\rangle\langle \mathbf{k}_j0_P|[\hat{\chi}^\dagger(\mathbf{b}')]^m|0_P0_T\rangle , \tag{6}$$

where $\mathbf{k}_j$ is the wave-number vector of a knocked-out target nucleon. The functions W_m are next related to the target response functions in the cylindrical geometry of the eikonal approximation.

COLLISION TERMS

In evaluating the collision terms W_m, we will assume an uncorrelated wave function for the target and plane waves for continuum states. The projectile motion is treated in the coherent approximation with the leading-order correction considered. We evaluate this term without the zero-range approximation [5], or factorization approximation [4], used previously in discussing proton-nucleus scattering.

The first collision term is written

$$W_1(\mathbf{b},\mathbf{b}',w)=\frac{A_P^2A_T}{(2\pi k_{NN})^2}\int d^2q\, d^2q'\, e^{i\mathbf{q}\cdot\mathbf{b}}e^{-i\mathbf{q}\cdot\mathbf{b}'}F(\mathbf{q})F(\mathbf{q}')f_{NN}(\mathbf{q})f_{NN}^\dagger(\mathbf{q}')\int\frac{d^2k}{(2\pi)^2}\delta(w-E_\mathbf{k})G_{0\mathbf{k}}(\mathbf{q})G_{\mathbf{k}0}^\dagger(\mathbf{q}') , \tag{7}$$

where F is the projectile ground-state form factor and $G_{0\mathbf{k}}$ the target transition form factor. We change variables as

$$\boldsymbol{\alpha}=\tfrac{1}{2}(\mathbf{q}+\mathbf{q}') , \tag{8}$$

$$\boldsymbol{\beta}=\mathbf{q}-\mathbf{q}' , \tag{9}$$

$$\mathbf{x}=\mathbf{s}-\mathbf{s}' , \tag{10}$$

$$\mathbf{y}=\tfrac{1}{2}(\mathbf{s}+\mathbf{s}') , \tag{11}$$

and also

$$\mathbf{R}=\mathbf{b}-\mathbf{b}' , \tag{12}$$

$$\mathbf{S}=\tfrac{1}{2}(\mathbf{b}+\mathbf{b}') , \tag{13}$$

such that

$$W_1(\mathbf{R},\mathbf{S},w)=\frac{A_P^2A_T}{(2\pi k_{NN})^2}\int d^2\alpha\, d^2\beta\, e^{i\boldsymbol{\alpha}\cdot\mathbf{R}}e^{i\boldsymbol{\beta}\cdot\mathbf{S}}\times A(\boldsymbol{\alpha}+\boldsymbol{\beta}/2)A^\dagger(\boldsymbol{\alpha}-\boldsymbol{\beta}/2)\times R_1(\boldsymbol{\alpha},\boldsymbol{\beta},w) , \tag{14}$$

where we have defined

$$A(\mathbf{q})=F(\mathbf{q})f_{NN}(\mathbf{q}) , \tag{15}$$

and the target response function is

$$R_1(\boldsymbol{\alpha},\boldsymbol{\beta},w)=\int\frac{d\mathbf{k}}{(2\pi)^2}\delta(w-E_\mathbf{k})G_{0\mathbf{k}}(\boldsymbol{\alpha}+\boldsymbol{\beta}/2)\times G_{\mathbf{k}0}^\dagger(\boldsymbol{\alpha}-\boldsymbol{\beta}/2) . \tag{16}$$

Following Krimm, Klar, and Pirner [4], we can formally treat the delta function in (16) by introducing a Fourier transform pair

$$R_1(\boldsymbol{\alpha},\boldsymbol{\beta},w)=\int\frac{dt}{2\pi}e^{iwt}\tilde{R}_1(\boldsymbol{\alpha},\boldsymbol{\beta},t) , \tag{17}$$

$$\tilde{R}_1(\boldsymbol{\alpha},\boldsymbol{\beta},t)=\int dw\, e^{-iwt}R_1(\boldsymbol{\alpha},\boldsymbol{\beta},w) . \tag{18}$$

Then

$$\tilde{R}_1(\boldsymbol{\alpha},\boldsymbol{\beta},t)=\int\frac{d\mathbf{k}}{(2\pi)^2}e^{-iE_\mathbf{k}t}G_{0\mathbf{k}}(\boldsymbol{\alpha}+\boldsymbol{\beta}/2)G_{\mathbf{k}0}^\dagger(\boldsymbol{\alpha}-\boldsymbol{\beta}/2) . \tag{19}$$

Treating the low-energy target nucleons nonrelativistically,

$$E_{\mathbf{k}}=\frac{\mathbf{k}^2}{2m_N}+\epsilon_{B_1}\ , \tag{20}$$

where ϵ_{B_1} is the binding energy. Equation (19) then becomes, assuming plane waves for the targets final state in $G_{0\mathbf{k}}$,

$$\tilde{R}_1(\boldsymbol{\alpha},\boldsymbol{\beta},t)=\int\frac{d\mathbf{k}}{(2\pi)^2}d\mathbf{x}\,d\mathbf{y}\,e^{-i\epsilon_{B_1}t}e^{-i\mathbf{k}^2t/2m_N}\times e^{i\boldsymbol{\alpha}\cdot\mathbf{x}}e^{i\boldsymbol{\beta}\cdot\mathbf{y}}e^{i\mathbf{k}\cdot\mathbf{x}}\Phi(\mathbf{y}+\mathbf{x}/2)\Phi^{\dagger}(\mathbf{y}-\mathbf{x}/2)\ , \tag{21}$$

where Φ is the single-particle wave function of the target ground state. Using Eqs. (21) and (17), we find

$$R_1(\boldsymbol{\alpha},\boldsymbol{\beta},w)=\begin{cases}\dfrac{m_N}{2\pi}\displaystyle\int d\mathbf{x}\,d\mathbf{y}\,e^{i\boldsymbol{\alpha}\cdot\mathbf{x}}e^{i\boldsymbol{\beta}\cdot\mathbf{y}}J_0([2m_N(w-\epsilon_{B_1})x^2]^{1/2}) \\ \qquad\times\Phi(\mathbf{y}+\mathbf{x}/2)\Phi^{\dagger}(\mathbf{y}-\mathbf{x}/2)\ \text{ for }\ w\ge\epsilon_{B_1}\ , \\ 0\ \text{ for }\ w<\epsilon_{B_1}\ .\end{cases} \tag{22}$$

The second collision term is more complicated because of the enumeration of projectile-target intermediate states that can occur. A first approximation is to keep only one-particle–one-hole excitations of the target (one for each inelastic scattering) and assume that the projectile remains in the ground state (coherent approximation). The coherent part of the second collision term is found using the notation of (15) to be

$$W_2(\mathbf{R},\mathbf{S},w)=\frac{A_P^4A_T^2}{4(2\pi k_{NN})^4}\int d^2\alpha_1d^2\alpha_2d^2\beta_1d^2\beta_2e^{i(\boldsymbol{\alpha}_1+\boldsymbol{\alpha}_2)\cdot\mathbf{R}}e^{i(\boldsymbol{\beta}_1+\boldsymbol{\beta}_2)\cdot\mathbf{S}}A(\boldsymbol{\alpha}_1+\boldsymbol{\beta}_1/2)A^{\dagger}(\boldsymbol{\alpha}_1-\boldsymbol{\beta}_1/2)$$
$$\times A(\boldsymbol{\alpha}_2+\boldsymbol{\beta}_2/2)A^{\dagger}(\boldsymbol{\alpha}_2-\boldsymbol{\beta}_2/2)R_2(\boldsymbol{\alpha}_1,\boldsymbol{\alpha}_2,\boldsymbol{\beta}_1,\boldsymbol{\beta}_2,w)\ , \tag{23}$$

where

$$R_2(\boldsymbol{\alpha}_1,\boldsymbol{\alpha}_2,\boldsymbol{\beta}_1,\boldsymbol{\beta}_2,w)=\begin{cases}\dfrac{m_N^2}{(2\pi)^2}\displaystyle\int d^2x_1d^2x_2d^2y_1d^2y_2e^{i\boldsymbol{\alpha}_1\cdot\mathbf{x}_1}e^{i\boldsymbol{\alpha}_2\cdot\mathbf{x}_2}e^{i\boldsymbol{\beta}_1\cdot\mathbf{y}_1}e^{i\boldsymbol{\beta}_2\cdot\mathbf{y}_2} \\ \qquad\times\Phi(\mathbf{y}_1+\mathbf{x}_1/2)\Phi^{\dagger}(\mathbf{y}_1-\mathbf{x}_1/2)\Phi(\mathbf{y}_2+\mathbf{x}_2/2)\Phi^{\dagger}(\mathbf{y}_2-\mathbf{x}_2/2) \\ \qquad\times\dfrac{2(w-\epsilon_{B_2})}{[2m_N(w-\epsilon_{B_2})(x_1^2+x_2^2)]^{1/2}}J_1\{[2m_N(w-\epsilon_{B_2})(x_1^2+x_2^2)]\}\ \text{ for }\ w\ge\epsilon_{B_2}\ , \\ 0\ \text{ for }\ w<\epsilon_{B_2}\ .\end{cases} \tag{24}$$

Using similar coordinate changes as described above, the mth-order collision term is found in the coherent approximation to be

$$W_m(\mathbf{R},\mathbf{S},w)=\frac{A_P^{2m}A_T^m}{(m!)^2(2\pi k_{NN})^{2m}}\int\prod_{j=1}^{m}\left[d^2\alpha_jd^2\beta_je^{i\boldsymbol{\alpha}_j\cdot\mathbf{R}}e^{i\boldsymbol{\beta}_j\cdot\mathbf{S}}A_j(\boldsymbol{\alpha}_j+\boldsymbol{\beta}_j/2)A_j^{\dagger}\left[\boldsymbol{\alpha}_j-\frac{\boldsymbol{\beta}_j}{2}\right]\right]$$
$$\times R_m(\boldsymbol{\alpha}_1,\ldots,\boldsymbol{\alpha}_m,\boldsymbol{\beta}_1,\ldots,\boldsymbol{\beta}_m,w)\ , \tag{25}$$

where

$$R_m(\boldsymbol{\alpha}_1,\ldots,\boldsymbol{\alpha}_m,\boldsymbol{\beta}_1,\ldots,\boldsymbol{\beta}_m,w)$$
$$=\frac{m_N^m}{(2\pi)^m}\int\prod_{j=1}^{m}[d^2x_jd^2y_je^{i\boldsymbol{\alpha}_j\cdot\mathbf{x}_j}e^{i\boldsymbol{\beta}_j\cdot\mathbf{y}_j}\Phi(\mathbf{y}_j+\mathbf{x}_j/2)\Phi^{\dagger}(\mathbf{y}_j-\mathbf{x}_j/2)]$$
$$\times\frac{2^{m-1}(w-\epsilon_{B_m})^{m-1}}{[2m_N(w-\epsilon_{B_m})\sum_{j=1}^{m}x_j^2]^{(m-1)/2}}J_{m-1}\left[2m_N(w-\epsilon_{B_m})\sum_{j=1}x_j^2\right]^{1/2}\ , \tag{26}$$

where $R_m=0$ for $w<\epsilon_{B_m}$. We next consider a simplified representation of the $m>1$ terms.

Assuming the target wave functions are forward peaked, we approximate

$$\frac{J_{m-1}[\xi_m(\sum_{j=1}^{m}x_j^2)^{1/2}]}{[\xi_m(\sum_{j=1}^{m}x_j^2)^{1/2}]^{m-1}}\cong\frac{1}{(m-1)!2^{m-1}}\prod_{j=1}^{m}J_0\left[\frac{\xi_mx_j}{2^{(m-1)/2}}\right]+O(\xi_m^4x_j^4)\ , \tag{27}$$

where

$$\xi_m=\sqrt{2m_N(w-\epsilon_{B_m})}\ , \tag{28}$$

such that

$$R_m(\alpha_1,\ldots,\alpha_m,\beta_1,\ldots,\beta_m,w)\simeq\frac{(w-\epsilon_{B_m})^{m-1}}{(m-1)!}\prod_{j=1}^{m}R_1\left[\alpha_j,\beta_j,\frac{\xi_m}{2^{(m-1)/2}}\right]\ , \tag{29}$$

$$W_m(\mathbf{R},\mathbf{S},w)=\frac{(w-\epsilon_{B_m})^{m-1}}{(m-1)!(m!)^2}\left[W_1\left[\mathbf{R},\mathbf{S},\frac{\xi_m}{2^{(m-1)/2}}\right]\right]^m\ . \tag{30}$$

A numerical test of the forward-peaked wave-function approximation is discussed below. We then have for the energy-loss spectra, in a coherent projectile model,

$$\left.\frac{d^2\sigma}{d\Omega dE_P'}\right|_{\text{in}}=\frac{k^2}{(2\pi)^2}\int d^2R\,d^2S\,e^{i\mathbf{q}\cdot\mathbf{R}}e^{i[\chi(\mathbf{R}+\mathbf{S}/2)-\chi^+(\mathbf{R}-\mathbf{S}/2)]}\sum_{m=1}^{A_T}\frac{(w-\epsilon_{B_m})^{m-1}}{(m-1)!(m!)^2}\left[W_1\left[\mathbf{R},\mathbf{S},\frac{\xi_m}{2^{(m-1)/2}}\right]\right]^m\ . \tag{31}$$

The coherent approximation assumes that the projectile remains in the ground-state throughout the scattering. The leading-order correction to the coherent terms occurs in W_2 and corresponds to the following replacement [16] for the projectile form factors in (23), which follows from using closure on intermediate states:

$$A_P^4F\left[\alpha_1+\frac{\beta_1}{2}\right]F\left[\alpha_1-\frac{\beta_1}{2}\right]F(\alpha_2+\beta_2/2)F(\alpha_2-\beta_2/2)\to A_P^2\{[F(2\alpha_1)+(A_P-1)F(\alpha_1+\beta_1/2)F(\alpha_1-\beta_2/2)]$$
$$\times[F(2\alpha_2)+(A_P-1)F(\alpha_2+\beta_2/2)F(\alpha_2-\beta_2/2)]\}\ . \tag{32}$$

Physically, the right-hand side of (32) represents the projectile dissociating in the intermediate state. Further modifications are necessary when correlation effects which are not included here are treated. Next, we consider model inputs and application of the above formalism.

CALCULATIONS AND RESULTS

We next discuss physical inputs necessary for evaluation of the cross sections of Eq. (31). We employ a two-body amplitude of the form

$$f_{NN}(\mathbf{q})=\frac{\sigma(\rho+i)k_{NN}}{4\pi}e^{-Bq^2/2}\ , \tag{33}$$

where, from Ref. [17], the isospin-averaged parameters are $\sigma=4.4$ fm^2, $\rho=-0.23$, and $B=0.23$ fm^2 at 1 GeV. For ^{4}He, a Gaussian wave function is used with a radius parameter [17] of $R_\alpha=1.33$ fm. For the elastic distortion phase χ, we use the more accurate charge form factor [18]

$$F_{\text{ch}}(\mathbf{q})=[1-(0.316q)^{12}]e^{-(0.681q)^2}\ , \tag{34}$$

which is corrected for finite proton size by the factor $\exp(-r_p^2q^2/6)$ with the proton radius $r_p=0.86$ fm.

In the Gaussian model, the response function is simply

$$R_1(\alpha,\beta,\xi)=2m_NR_\alpha^2e^{-R_\alpha^2\beta^2/4}e^{-R_\alpha^2\alpha^2}e^{-R_\alpha^2\xi^2}I_0(2R_\alpha^2\alpha\xi)\ , \tag{35}$$

where I_0 is the zeroth-order modified Bessel function.

In evaluating the cross section, we make one further approximation by expanding the elastic distortion phase about $\mathbf{R}=0$ and keeping just the first two terms:

$$\chi(\mathbf{R}+\mathbf{S}/2)-\chi^+(\mathbf{R}-\mathbf{S}/2)=-2\,\text{Im}\chi(\mathbf{S})-i\mathbf{R}\cdot\nabla_S\chi(\mathbf{S})\ , \tag{36}$$

where the effect of the second term in (36) allows for momentum to be transferred in elastic scattering [19]. For comparisons to the data of Ref. [7], we note the relationship

$$\left.\frac{d^2\sigma}{d\Omega\,dP_P'}\right|_{\text{in}}=\frac{P_P'}{E_P'}\left.\frac{d^2\sigma}{d\Omega\,dE_P'}\right|_{\text{in}}\ . \tag{37}$$

Before discussing our comparisons to the experiment of Banaigs *et al.* [7], we emphasize the simplicity of our inputs for the ^{4}He ground-state wave function. Our comparisons thus focus on the magnitude of the various terms and their effect on the shapes of the spectra. We also note that a previous study [15] suggested an important role for scattering on subclusters in ^{4}He, which is not treated here. Scattering on subclusters does appear here in the multiple-scattering terms. However, for a light target such as ^{4}He, the replacement of the single-particle wave functions by cluster overlap functions is needed to describe properly this effect.

In Fig. 1 we illustrate the accuracy of the approximation of Eq. (30) for the term W_2 for α-α scattering at 3.63°. This angle is chosen because here the contribution from W_2 is large in comparison to the other collision terms. The dotted line is obtained using Eq. (30), and the dash line is the exact result using Eq. (23). Also shown are corrections for internal excitation of the projectile, with the solid line the exact result and the dot-dashed line

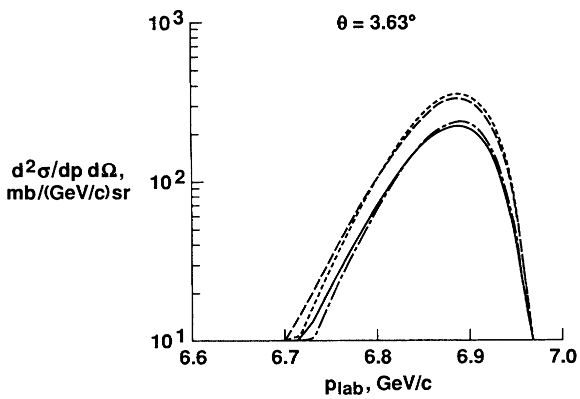

FIG. 1. Comparison of contributions of second collision term W_2 to the cross section using various approximations for α-^{4}He scattering at 3.63°. The solid line is the exact incoherent result, the dot-dashed line is the incoherent result with a forward-peaked wave-function approximation, the dashed line is the exact coherent result, and the dotted line is the coherent result with a forward-peaked wave-function approximation.

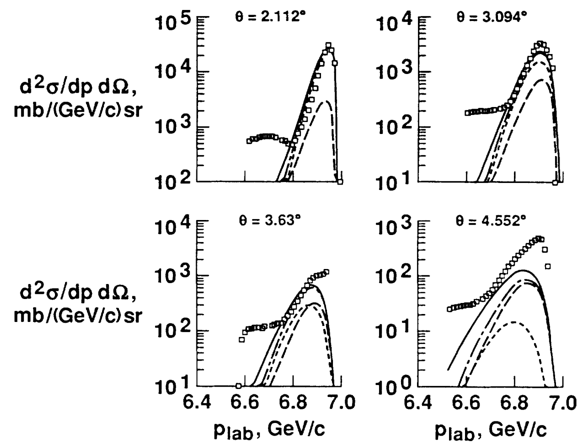

FIG. 2. Momentum spectra of α particles in α-^{4}He collisions at 1 A GeV for scattering angles of 2.112° ($q=1.31$ fm^{-1}), 3.094° ($q=1.92$ fm^{-1}), 3.63° ($q=2.25$ fm^{-1}), and 4.552° ($q=2.82$ fm^{-1}). Experimental data are from Ref. [7]. The dotted line is the first collision term, the dashed line is the second collision term, the dot-dashed line is the sum of the first and second collision terms and the solid line includes the third collision term.

the forward-peak wave-function approximation. Incoherent effects are shown to reduce significantly the second collision term. The reduction in the cross section that occurs through incoherent contributions from the projectile suggests that correlations effects in the projectile may be important.

Theoretical calculations for quasielastic α-^{4}He scattering at 1 GeV/nucleon are compared with experiment [7] in Fig. 2 for several scattering angles. The calculations shown are made with the approximation of (31), where the dotted line is the first collision term, the dashed line the second collision term, the dot-dashed the sum of the first and second terms, and the solid line the sum through the third collision term. For consistency, we show only the coherent contributions since we have not formulated the corrections for incoherent projectile motion beyond W_2. The multiple-scattering structure is apparent with single inelastic collisions dominating at a small momentum transfers and the higher-order contributions increasing in importance with q. In Fig. 2 the positions of the peaks in the cross sections as a function of energy loss for the first and second collision terms can be compared as the scattering angle increases. At $\theta=3.63°$ and 4.552° in Fig. 2, the second collision term is dominating. The position of the quasielastic peak no longer appears at $w=q^2/2m$, as the energy loss is shared between at least two scatterings and, as a result, is shifted to smaller values. This effect keeps the position of the theoretical peak in good agreement with the experiment. The strengths of the distributions compare fairly well with experiment except at the largest momentum transfers, where, at lower values of momentum, energy losses sufficient for pion production [7] are reached, which is not included in our calculations. The discrepancy between experiment and calculations increases for the larger angle data of Ref. [7] (not shown) and is attributed to our use of a Gaussian wave function for the ^{4}He ground state and the neglect of pion production.

CONCLUSION

We have used a coupled-channel representation of the nucleus-nucleus scattering amplitude in the eikonal approximation to develop a multiple collision series for describing the quasielastic peak in nucleus-nucleus collisions. Leading-order corrections for internal excitation of the projectile were discussed and found to make significant corrections to double scatterings in α-^{4}He collisions. A forward-peaked wave-function approximation was found to be quite accurate and to lead to considerable simplicity in the calculations. Multiple inelastic collision contributions were shown to provide the correct positioning with energy loss of the quasielastic peak in comparison to experiments for 4 GeV α-^{4}He scattering. Future calculations should use more realistic ground-state wave functions than the Gaussian model used here and should include higher-order corrections for incoherent projectile motion.

[1] R. J. Glauber and G. M. Matthiae, Nucl. Phys. **B21**, 135 (1970).
[2] R. J. Glauber, O. Kofoed-Hansen, and B. Margolis, Nucl. Phys. **B30**, 220 (1971).
[3] M. Thies, Ann. Phys. (N.Y.) **123**, 411 (1979).
[4] W. Krimm, A. Klar, and H. J. Pirner, Nucl. Phys. **A367**, 333 (1981).
[5] R. O. Smith and S. J. Wallace, Phys. Rev. C **32**, 164 (1985).
[6] J. Duflo *et al.*, Nucl. Phys. **A356**, 427 (1981).

[7] J. Banaigs *et al.*, Phys. Rev. C **35**, 1416 (1987).
[8] I. Bergquist *et al.*, Nucl. Phys. **A469**, 648 (1987).
[9] T. Fujita and J. Hüfner, Phys. Lett. **87B**, 327 (1979).
[10] A. Malecki, P. Picozza, and L. Satta, Phys. Lett. **136B**, 319 (1984).
[11] F. A. Cucinotta, G. S. Khandelwal, L. W. Townsend, and J. W. Wilson, Phys. Lett. B **223**, 127 (1989).
[12] J. W. Wilson, Ph.D. thesis, College of William and Mary, 1974.
[13] J. W. Wilson and L. W. Townsend, Can. J. Phys. **59**, 1569 (1981).
[14] W. Czyz and L. W. Maximon, Ann. Phys. (N.Y.) **52**, 59 (1969).
[15] J. Duflo, Phys. Rev. C **36**, 1425 (1987).
[16] F. A. Cucinotta, L. W. Townsend, J. W. Wilson, and G. S. Khandelwal, NASA Technical Report No. 3026, 1990.
[17] V. Franco and Y. Yin, Phys. Rev. Lett. **55**, 1059 (1985).
[18] J. S. McCarthy, I. Sick, and R. R. Whitney, Phys. Rev. C **15**, 1396 (1977).
[19] F. A. Cucinotta, L. W. Townsend, and J. W. Wilson, J. Phys. G **18**, 889 (1992).